Check for updates

Geophysical Research Letters

RESEARCH LETTER
10.1029/2021GL097372

Special Section:
Southern Ocean and Climate: Biogeochemical and Physical Fluxes and Processes

New Estimates of Southern Ocean Annual Net Community Production Revealed by BGC-Argo Floats

Jiaoyang Su[1,2], Christina Schallenberg[1,3], Tyler Rohr[3], Peter G. Strutton[1,2], and Helen E. Phillips[1,3,4]

[1]Institute for Marine and Antarctic Studies, University of Tasmania, Hobart, TAS, Australia, [2]Australian Research Council Center of Excellence for Climate Extremes, University of Tasmania, Hobart, TAS, Australia, [3]Australian Antarctic Program Partnership, Hobart, TAS, Australia, [4]Australian Center for Excellence in Antarctic Science, Institute for Marine and Antarctic Studies, University of Tasmania, Hobart, TAS, Australia

Key Points:

- A novel approach was developed to estimate annual net community production (ANCP) by integrating oxygen drawdown from all available biogeochemical Argo oxygen profiles
- Total basin-integrated ANCP in the Southern Ocean was 3.89 GT C year^{-1}
- We found 15% of measured dissolved oxygen drawdown occurred above 100 m, but below the euphotic zone, and 14% occurred below 500 m

Supporting Information:

Supporting Information may be found in the online version of this article.

Correspondence to:

J. Su,
jiaoyang.su@utas.edu.au

Citation:

Su, J., Schallenberg, C., Rohr, T., Strutton, P. G., & Phillips, H. E. (2022). New estimates of Southern Ocean annual net community production revealed by BGC-Argo floats. *Geophysical Research Letters*, *49*, e2021GL097372. https://doi.org/10.1029/2021GL097372

Received 12 DEC 2021
Accepted 6 JUL 2022

Author Contributions:

Conceptualization: Jiaoyang Su, Christina Schallenberg, Tyler Rohr, Peter G. Strutton, Helen E. Phillips
Data curation: Jiaoyang Su
Formal analysis: Jiaoyang Su, Christina Schallenberg, Tyler Rohr, Peter G. Strutton
Funding acquisition: Peter G. Strutton

© 2022. The Authors.
This is an open access article under the terms of the Creative Commons Attribution-NonCommercial-NoDerivs License, which permits use and distribution in any medium, provided the original work is properly cited, the use is non-commercial and no modifications or adaptations are made.

Abstract Using an expanding Southern Ocean fleet of biogeochemical Argo (BGC-Argo) floats, we developed a novel approach to estimate annual net community production (ANCP) by integrating subsurface oxygen drawdown from all available BGC-Argo oxygen profiles. Our results suggest that, on average, 14% of remineralization occurs between 500 and 1,000 m and 15% occurs between the euphotic depth and 100 m. Using the improved methodology, we estimated total basin-integrated ANCP in the Southern Ocean to be 3.89 GT C year^{-1} suggesting a more important role for the Southern Ocean in regulating oceanic carbon storage, atmospheric CO_2 exchange and climate than previously assumed.

Plain Language Summary Annual net community production (ANCP) is the amount of biologically produced carbon available for export to the deep ocean. We developed a novel approach to estimate ANCP in the Southern Ocean, using robotic floats. Using our improved method, total basin-integrated ANCP in the Southern Ocean was 3.89 GT C year^{-1}. These higher estimates could suggest a more important role for the Southern Ocean in regulating oceanic carbon storage, atmospheric CO_2 exchange and climate than previously thought.

1. Introduction

Oceanic net primary production (NPP) accounts for half of global carbon fixation (Falkowski, 2012). The fraction of NPP that sinks out of the surface contributes to the oceanic sink for atmospheric CO_2 (Sabine et al., 2004; Sarmiento & Gruber, 2002). Roughly 97% of exported organic material is respired by bacteria and zooplankton before reaching 1,000 m (Giering et al., 2014; Steinberg et al., 2008). However, accurate estimates of the magnitude of the Southern Ocean biological carbon sink are limited and subject to ongoing debate (Arteaga et al., 2019; Bender & Jönsson, 2016; Hennon et al., 2016; Johnson et al., 2017; Lourey & Trull, 2001; MacCready & Quay, 2001; Martz et al., 2008; McNeil & Tilbrook, 2009; Munro et al., 2015; Riser & Johnson, 2008; Shadwick et al., 2015).

At steady state, over long enough time and space scales (>1,000 km and seasons), net community production (NCP) is the amount of carbon fixed during photosynthesis that is not remineralized in the surface layer and remains available for export to depth (Brix et al., 2006; Emerson, 2014). Here, we define the surface layer as the greater of the euphotic zone and mixed layer. Annual net community production (ANCP) is the depth-integrated NCP over a year. Typically, ANCP is estimated using chemical tracer budgets in the surface ocean (Emerson, 2014). Nowadays, ANCP and export can be measured using biogeochemical Argo (BGC-Argo) floats (Bushinsky & Emerson, 2018; Johnson et al., 2017; Llort et al., 2018; Nicholson et al., 2008; Riser & Johnson, 2008; Williams et al., 2018; Yang et al., 2017), but there is no consensus on the most robust depth range to integrate across. Most remineralization occurs between 100 and 1,000 m (Honjo et al., 2000), but previous work has used different depth ranges for ANCP. For example, Arteaga et al. (2019) used 100–500 m and Hennon et al. (2016) used 70 m to the depth where the mean respiration rate reached zero.

Two recent estimates of ANCP based on nitrate (Johnson et al., 2017) and oxygen drawdown (Arteaga et al., 2019) extrapolated results from individual BGC-Argo floats. However, the increasing number of BGC-Argo floats deployed in the Southern Ocean has enabled us to combine all available floats to better quantify mean oxygen

Investigation: Jiaoyang Su, Christina Schallenberg, Tyler Rohr, Peter G. Strutton, Helen E. Phillips
Methodology: Jiaoyang Su, Christina Schallenberg, Tyler Rohr, Peter G. Strutton
Resources: Jiaoyang Su, Peter G. Strutton
Supervision: Christina Schallenberg, Tyler Rohr, Peter G. Strutton, Helen E. Phillips
Validation: Jiaoyang Su, Christina Schallenberg, Tyler Rohr, Peter G. Strutton
Visualization: Jiaoyang Su, Christina Schallenberg, Tyler Rohr, Peter G. Strutton, Helen E. Phillips
Writing – original draft: Jiaoyang Su
Writing – review & editing: Jiaoyang Su, Christina Schallenberg, Tyler Rohr, Peter G. Strutton, Helen E. Phillips

drawdown at depth at the basin scale. Our study provides a novel approach to a bulk analysis of ANCP and reveals its spatial variability in three basins and four frontal regions across the Southern Ocean.

2. Data and Methods

2.1. BGC-Argo Float Data

BGC-Argo floats measure depth, temperature and salinity and up to six additional properties: dissolved oxygen (DO), pH, dissolved nitrate, downwelling irradiance, chlorophyll fluorescence and particulate backscatter (Bittig et al., 2019). We used all BGC-Argo floats spanning January-2003–October-2020 south of 40°S that measured DO. We also included all floats spanning September-2010–October-2020 that measured chlorophyll to support our analysis. BGC-Argo float data were obtained from ftp.ifremer.fr/ifremer/argo/dac/in November-2020. The vertical sampling interval was about 10 m from the surface to 400 m but can be as sparse as 50 m from 400 to 2,000 m. We linearly interpolated DO every 1 m.

2.2. Quality Control

Dissolved oxygen, temperature, salinity and pressure are well quality controlled in the BGC-Argo floats delayed-mode data set (Bittig et al., 2019). Following Su et al. (2021), we applied a range test (Barbieux et al., 2018), despiking and a non-photochemical quenching correction to the raw chlorophyll data (Xing et al., 2012; Section 1 in Supporting Information S1). We removed all profiles with a deepest sampling depth shallower than 1,500 m because the dynamic height anomaly used to locate a profile relative to frontal boundaries is computed between 500 and 1,500 dbar (see below).

2.3. Front Definition

We defined four frontal zones as the Subantarctic Zone (SAZ), from 40°S to the subantarctic front (SAF); Polar Frontal Zone (PFZ), between the SAF and the polar front (PF); Antarctic Zone (AZ), between the PF and the southern Antarctic Circumpolar Current front (SACCF); and Southern Zone (SZ), from the SACCF to the mean winter maximum sea ice extent (Talley, 2011). Ice extent was defined by data from the National Snow and Ice Data Center following Cavalieri et al. (1996), updated yearly (Phil Reid, personal communication). Methods for dynamic height anomaly calculation (McDougall & Barker, 2011) and best defining front locations are provided in Section 2 of Supporting Information S1.

2.4. Estimation of ANCP

Temporal variability in DO (dDO/dt) is controlled by the physical processes of advection, diffusion, and gas exchange, in addition to the biological processes of photosynthesis and remineralization (Arteaga et al., 2019). During spring and summer, biological processes dominate observed dDO/dt (Hennon et al., 2016). Gas exchange is negligible below the mixed layer depth (MLD), where water remains out of contact with the atmosphere, and photosynthesis approaches zero below the euphotic zone (and MLD), where light is unavailable. The observed change in oxygen below the surface layer during the productive season can be attributed entirely to remineralization, and remineralization at a given depth ($R(z)$) can be calculated as

$$R(z) = -0.69 \times d[\mathrm{DO}(z)/\mathrm{dt}] \quad (1)$$

Where 0.69 is the respiratory quotient for organic matter remineralization (117 C:170 mol O_2; Anderson & Sarmiento, 1994).

We took the mean of all float observations of DO for each day of the year on each depth level. The productive period (D_{prod}), was defined as the section of the seasonal cycle where DO decreases and where all annual particle export and remineralization is assumed to occur (Arteaga et al., 2019). At each depth, $D_{\mathrm{prod}}(z)$ was found by smoothing DO using Loess filtering with a span of 0.25 (approximately 90 days) and locating the late winter DO maximum and the summer-autumn minimum (see Section 3 in Supporting Information S1 for details). By dynamically defining D_{prod} at each depth based on the measured drawdown of oxygen, we account for both anomalously long productive periods and the temporal offset between ANCP at the surface and where it is eventually remineralized.

19448007, 2022, 15, Downloaded from https://agupubs.onlinelibrary.wiley.com/doi/10.1029/2021GL097372 by National Health And Medical Research Council, Wiley Online Library on [18/01/2024]. See the Terms and Conditions (https://onlinelibrary.wiley.com/terms-and-conditions) on Wiley Online Library for rules of use; OA articles are governed by the applicable Creative Commons License

The mean remineralization rate at a given depth ($\overline{R(z)}$) was estimated as the slope of a linear regression fit to the unsmoothed DO data within $D_{prod}(z)$ (Arteaga et al., 2019). To estimate ANCP (mol C m^{-2} $year^{-1}$), we integrate the product of $\overline{R(z)}$ (mol C d^{-1}) and $D_{prod}(z)$ (d) across the depth range of interest:

$$\mathrm{ANCP} = \int_{\mathrm{lowerlimit}}^{\mathrm{upper\,limit}} \overline{R(z)} \times D_{\mathrm{prod}}(z)\mathrm{dz} \tag{2}$$

Depths with less than 20 data points or with slopes that were statistically insignificant from zero were excluded.

In our primary calculation of ANCP we define the lower limit of integration as 1,000 m and the upper limit as Z_{surf}, which is the greater of the euphotic depth (Z_{eu}) and mixed layer depth (Z_{MLD}). Z_{surf} is mostly equal to Z_{eu} because MLD was shallower than Z_{eu} and Z_{eu} was shallower than 100 m during most of D_{prod}. For comparisons with other studies and definitions of ANCP, we additionally consider several alternate depth windows: 100–1,000, Z_{MLD}-1000 and Z_{eu}-1000. In all cases, we stop integrating at the MLD if it is deeper than the nominal upper limit to avoid considering water in contact with the atmosphere. Any depth level where no significant net remineralization was detected was treated as zero in the integration. Z_{eu} is defined by the 1% light level, calculated as a function of chlorophyll (Morel & Maritorena, 2001, Section 4 in Supporting Information S1). The mixed layer depth was calculated based on the 0.03 kg m^{-3} potential density criterion relative to 10 m (Holte & Talley, 2009):

$$\sigma(\mathrm{MLD}) - \sigma(10\mathrm{m}) > 0.03\,\mathrm{kg\,m^{-3}} \tag{3}$$

Spatially integrated carbon export (mol C $year^{-1}$) was estimated as

$$\mathrm{Carbon\,export} = \mathrm{ANCP}_{100} \times \mathrm{Area} \tag{4}$$

where Area is, for example, the area of the SAZ in the Indian sector of the Southern Ocean. $ANCP_{100}$ is the ANCP estimated from 100 to 1,000 m. We included this depth range as well as the MLD and Z_{surf} upper boundaries to make our results comparable to other studies, which most frequently define export through the 100 m depth horizon, and to highlight the depth range where most ANCP occurs. Both ANCP and carbon export were estimated for all three basins of the Southern Ocean (Indian, Atlantic, Pacific) and for the four frontal regions described in Section 2.3.

Errors were calculated using the 90% confidence interval for $\overline{R(z)}$, that is, integrating ANCP using the maximum and minimum $\overline{R(z)}$ in that confidence interval at each depth. Errors were assumed to propagate linearly.

2.5. Export Production and Efficiency

Export efficiency, also called the e-ratio, is the fraction of NPP exported through a depth level (Laufkötter et al., 2016). For comparison with other studies, we defined export production (EP) as the particle flux through 100 m, which is assumed equal to ANCP calculated from 100 to 1,000 m ($ANCP_{100}$) and divided by 0.97 to account for 3% of particles that sink past 1,000 m (Christina & Passow, 2007).

$$e - \mathrm{ratio} = \mathrm{EP}/\mathrm{NPP} = \frac{\mathrm{ANCP}_{100}}{0.97}/\mathrm{NPP} \tag{5}$$

NPP was estimated from the Carbon-based Production Model 8 day product (Westberry et al., 2008) using Moderate Resolution Imaging Spectroradiometer r-2018 results (http://orca.science.oregonstate.edu/1080.by.2160.8day.hdf.cbpm2.m.php). NPP was averaged over the same spatial and temporal bins as used for the $ANCP_{100}$ estimates.

3. Results

3.1. Oxygen Profiles in the Southern Ocean

There were 54,599 quality-controlled DO profiles in the Southern Ocean south of 40°S spanning Janaury-2003–October-2020. After filtering out shallow profiles (see Section 2.2), we retained 25,512 profiles, of which 8,341, 12,712 and 4,459 were in the Indian, Pacific and Atlantic sectors respectively (Figure 1). Roughly half of the profiles were found in the SAZ, while only 2,462 profiles were found in the SZ.

19448007, 2022, 15, Downloaded from https://agupubs.onlinelibrary.wiley.com/doi/10.1029/2021GL097372 by National Health And Medical Research Council, Wiley Online Library on [18/01/2024]. See the Terms and Conditions (https://onlinelibrary.wiley.com/terms-and-conditions) on Wiley Online Library for rules of use; OA articles are governed by the applicable Creative Commons License

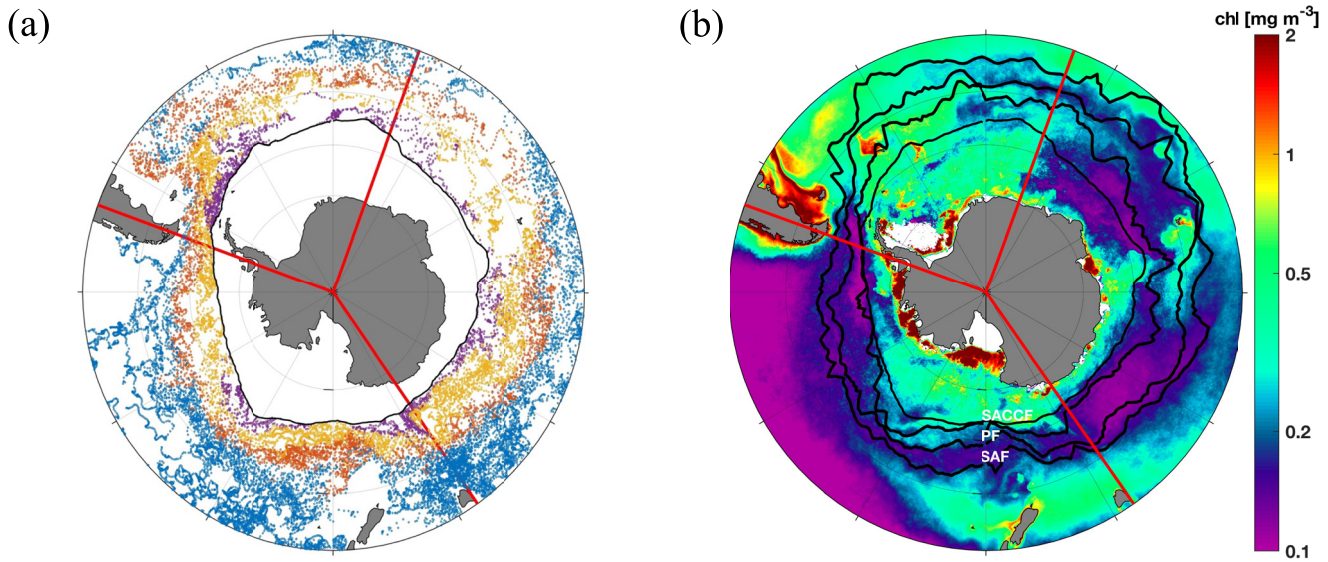

Figure 1. (a) Oxygen profiles in the Southern Ocean in four frontal regions: Subantarctic Zone (blue), Polar Frontal Zone (orange), Antarctic Zone (yellow), and Southern Zone (purple). Basin boundaries are marked with red lines. The southern boundary of the data set was the maximum sea ice edge (solid line). (b) Average summer (December, January, February) chlorophyll (chl) concentration from 1997 to 2019. Chlorophyll data were from SeaWiFS (1997–2010) and Moderate Resolution Imaging Spectroradiometer-Aqua (2002–2019), averaged where there is overlap (https://oceancolor.gsfc.nasa.gov). Moving north to south, the subantarctic front (SAF), polar front (PF), southern Antarctic Circumpolar Current front (SACCF), and the maximum sea ice edge are marked with black lines.

3.2. Seasonal Cycles of Chlorophyll and DO

The seasonal cycles of mean mixed layer chlorophyll and subsurface dDO/dt indicate that biomass maxima in the mixed layer are followed by remineralization (negative dDO/dt) at depth, as would be expected (Figure 2). Time-depth sections of dDO/dt illustrate the depth range where remineralization is dominant, which we determined to be to 1,000 m and made use of in the ANCP calculation.

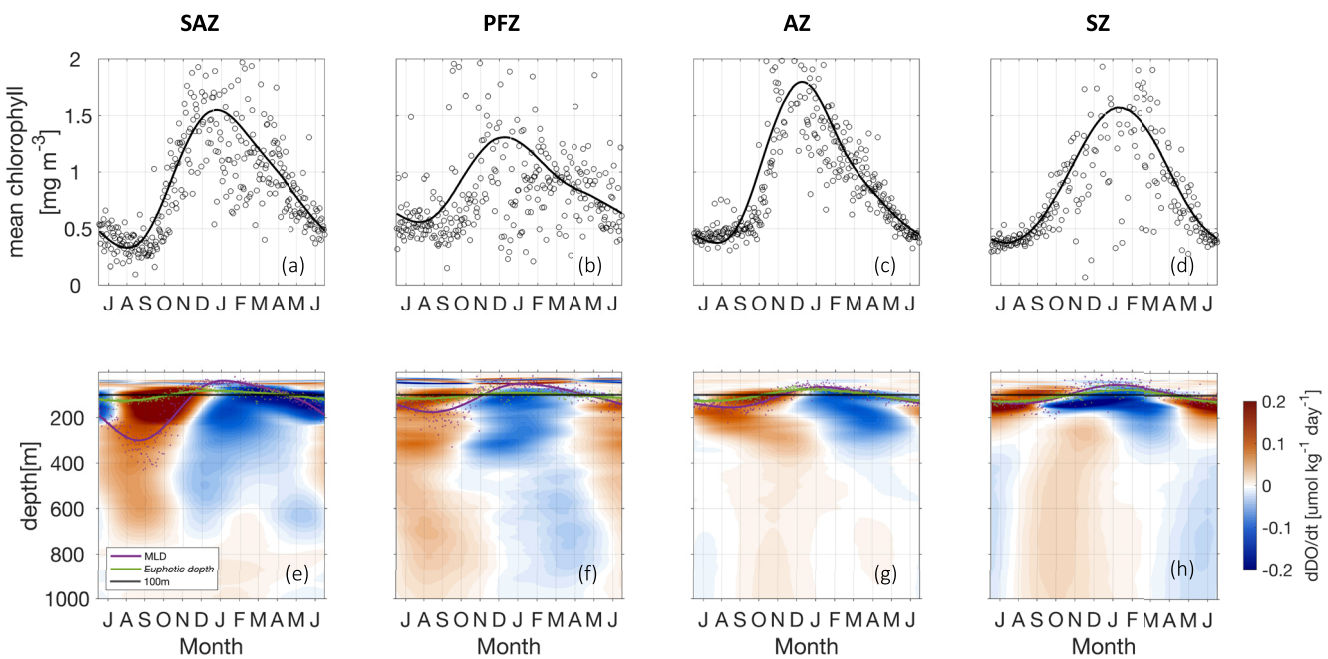

Figure 2. Seasonal cycles of (a–d) mean mixed layer chlorophyll and (e–h) dDO/dt, for the Indian sector of the Southern Ocean. Mixed layer depth (MLD; purple), Z_{eu} (green) and 100 m (black) are plotted on top of dDO/dt. The white area left between periods of positive and negative dDO/dt in e–h delineates the bounds of D_{prod}, which vary with depth. Details of data visualization are given in Section 5 of Supporting Information S1.

19448007, 2022, 15, Downloaded from https://agupubs.onlinelibrary.wiley.com/doi/10.1029/2021GL097372 by National Health And Medical Research Council, Wiley Online Library on [18/01/2024]. See the Terms and Conditions (https://onlinelibrary.wiley.com/terms-and-conditions) on Wiley Online Library for rules of use; OA articles are governed by the applicable Creative Commons License

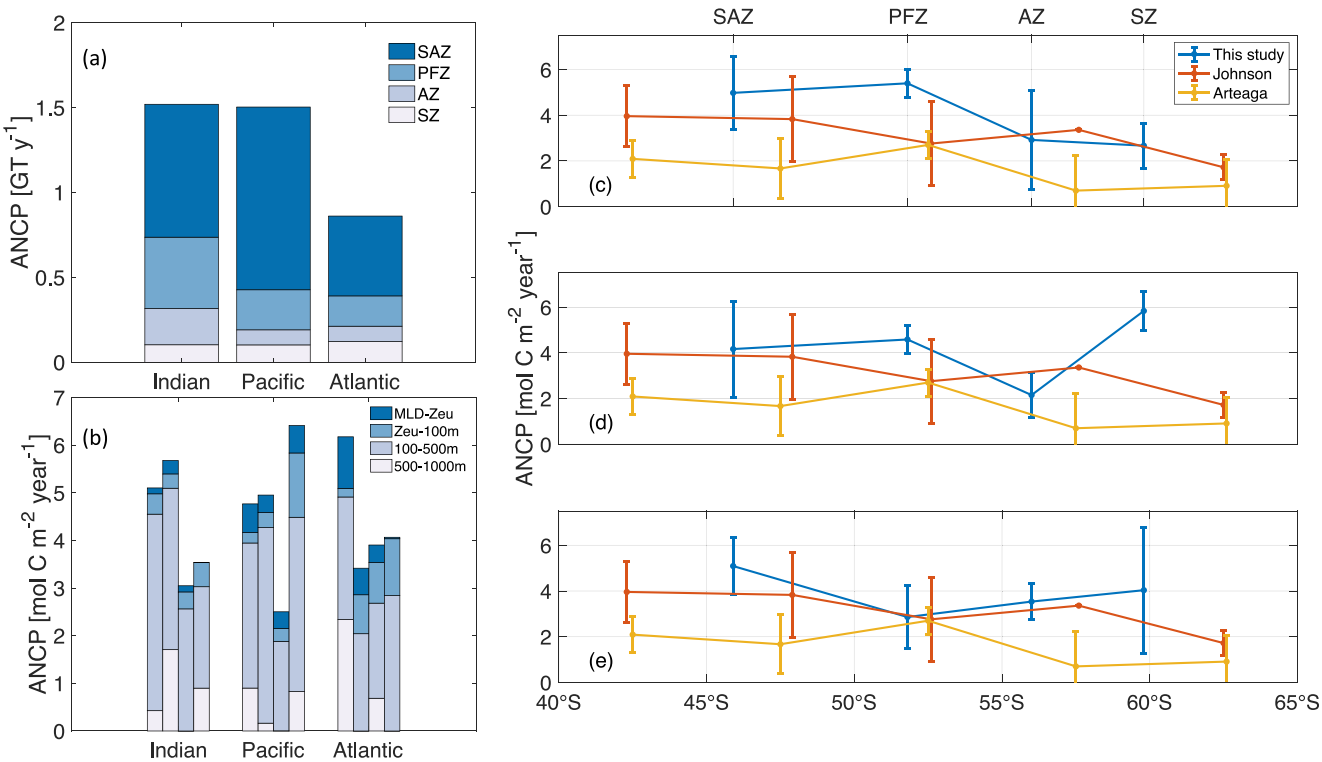

Figure 3. (a) Frontal variability in integrated annual net community production (ANCP) for each basin. (b) Regional depth-resolved ANCP in each basin and frontal region. For each sector, from left to right, each bar represents the Subantarctic Zone (SAZ), PFZ, Antarctic Zone (AZ) and Southern Zone (SZ). Note that mixed layer depth (MLD)-Z_{eu} was negative in the SZ of the Indian sector and is thus not shown. (c–e) Comparisons of regional variability in ANCP (with error bars) between Johnson et al. (2017), Arteaga et al. (2019) and this study in the Indian, pacific and Atlantic sectors respectively. Note, subplots (a and c–e) show ANCP estimated between Z_{surf} (mostly equal to Z_{eu}) and 1,000 m from our study but subplot (b) additionally includes what was measured between MLD and Z_{eu} in dark blue.

Qualitatively, these seasonal cycles exhibit minor differences between basins. Figure 2 shows the Indian sector as an example. Mean mixed layer chlorophyll was highest in summer and lowest in winter. Seasonal variability in remineralization rates was evident in subsurface dDO/dt, and mostly consistent with depth except in the SZ, where seasonal cycles from the base of the mixed layer/euphotic zone to 300 m were opposite to the cycles from 300 to 1,000 m. There were delays of approximately 1–2 months in the response of dDO/dt below the surface layer to the variability of mean mixed layer chlorophyll in the SAZ and AZ but not in the PFZ and SZ.

3.3. ANCP Estimates

Basin-integrated ANCP in the Southern Ocean (from Z_{surf} to 1,000 m and from 40°S to the maximum sea ice zone) was 3.89 GT C year^{-1} (Figure 3). Regionally, integrated ANCP was highest in the Indian (1.53 GT C year^{-1}), followed by the Pacific (1.50 GT C year^{-1}) and Atlantic (0.86 GT C year^{-1}). Normalizing by area, ANCP (mol C m^{-2} year^{-1}) was 2.67–5.40, 2.15–5.84 and 2.86–5.09 mol C m^{-2} year^{-1} in the Indian, Pacific and Atlantic sectors, respectively, where the ranges indicate variability across frontal regions (Figure 3b). Total ANCP, as well as ANCP in each basin and frontal region is summarized in Section 6, Table S3 of Supporting Information S1. We calculated ANCP values that were mostly higher than Johnson et al. (2017) and Arteaga et al. (2019) but errors were comparable (Figures 3c–3e).

Depending on the region, only 42%–84% percent of estimated Southern Ocean ANCP was based on remineralization occurring between 100 and 500 m, while 3%–29% occurred in the surface ocean, above 100 m but below the euphotic depth, and 0%–38% occurred between 500 and 1,000 m. Averaged across the Southern Ocean, remineralization rates decrease rapidly with depth but remain above 0.008 μmol kg^{-1} day^{-1} through the lower mesopelagic zone and down to 1,000 m (Figure S3 in Supporting Information S1). However, one third of the regions considered do not experience any measurable remineralization below 500 m (Figure 3b). Regarding the different upper depth horizons, ANCP calculated with an upper bound of 100 m was usually smallest, followed

19448007, 2022, 15, Downloaded from https://agupubs.onlinelibrary.wiley.com/doi/10.1029/2021GL097372 by National Health And Medical Research Council, Wiley Online Library on [18/01/2024]. See the Terms and Conditions (https://onlinelibrary.wiley.com/terms-and-conditions) on Wiley Online Library for rules of use; OA articles are governed by the applicable Creative Commons License

19448007, 2022, 15, Downloaded from https://agupubs.onlinelibrary.wiley.com/doi/10.1029/2021GL097372 by National Health And Medical Research Council, Wiley Online Library on [18/01/2024]. See the Terms and Conditions (https://onlinelibrary.wiley.com/terms-and-conditions) on Wiley Online Library for rules of use; OA articles are governed by the applicable Creative Commons License

by euphotic depth and MLD. This is consistent with the fact that MLD was shallower than Z_{eu} and Z_{eu} was shallower than 100 m during most of D_{prod} in most locations. Where this was not the case, ANCP estimated with an upper depth horizon of Z_{eu} was larger than if MLD was used because deep MLDs occasionally shorten the depth horizon for integration.

4. Discussion

This study developed a novel approach to calculate ANCP in the Southern Ocean using oxygen drawdown from aggregated rather than individual BGC-Argo floats. Spatial variability of ANCP was estimated in three basins, four frontal regions and over several depth ranges and compared with previous findings. Total basin-integrated ANCP in the Southern Ocean from this study is 3.89 GT C year^{-1}.

4.1. Comparison With Other Studies

In the Indian and Pacific sectors, ANCP is high in the SAZ and PFZ and decreases toward the AZ, which is consistent with the spatial variability of ANCP (Arteaga et al., 2019; Johnson et al., 2017) and particulate organic carbon (POC) export at 100 m (Henley et al., 2020). However, in the Pacific sector, there is another increase toward the SZ which was not shown in previous studies. In the Atlantic sector, ANCP is highest in SAZ, decreases toward the PFZ and then increases slightly toward the AZ. Such little variability in the south is roughly consistent with the variability of surface chlorophyll from satellites, indicating surface biomass could be the major factor controlling ANCP in the Atlantic sector.

Overall, our estimates of ANCP in almost all locations are greater than previous estimates based on nitrate drawdown (Johnson et al., 2017) or oxygen drawdown (Arteaga et al., 2019) from individual floats. There are two differences between our study and Arteaga et al. (2019). First, we integrated from Z_{surf} to 1,000 m, while Arteaga et al. (2019) used 100–500 m, leading to higher ANCP in our study by up to 3.17, 5.12 and 3.32 mol C m^{-2} year^{-1} in the Indian, Pacific and Atlantic sectors, respectively, depending on the frontal zone (Figures 3c–3e). However, even when integrated across an identical depth range (100–500 m), our estimates exceed those of Arteaga et al. (2019) by up to 2.32, 2.95 and 2.13 mol C m^{-2} year^{-1} in the Indian, Pacific and Atlantic sector, respectively, depending on the frontal zone (Section 7 in Supporting Information S1). This suggests a second, methodological explanation. Arteaga et al. (2019) looked at 123 individual floats (about 10 floats per region on average) because they were limited to floats with life spans of more than 1 year. In contrast, we created an ensemble seasonal cycle comprised of all available floats in a given region (about 23 floats per region on average). By using a much larger sample size, rather than spatially extrapolating from a smaller number of floats, our estimates may better represent basin scale mean ANCP, particularly considering the largely overlapping uncertainties in data collection. However, there is no particular reason why this would lead to an overestimation or underestimation of ANCP compared to Arteaga et al. (2019).

There are also at least two possible reasons for the difference between Johnson et al. (2017) and our study. Firstly, nitrate input to the mixed layer from the deep ocean by advection or mixing or both could lead to underestimation in Johnson et al. (2017), who used vertically integrated nitrate drawdown between summer and winter. Secondly, and similar to the issue raised above, we used 25,512 profiles compared with approximately 495 profiles (from 31 floats) in Johnson et al. (2017), so their regional estimates may depend strongly on how representative the floats were for each region.

Other studies of ANCP in the Southern Ocean have been based on measurements from ships or moorings (Lourey & Trull, 2001; McNeil & Tilbrook, 2009; Munro et al., 2015), models (Bender & Jönsson, 2016), or very few BGC-Argo floats (Hennon et al., 2016; Martz et al., 2008; Riser & Johnson, 2008). All of these studies were limited to one–three locations and lacked spatial representation. Where our ANCP estimates overlap in space with previous work (all of those cited above except Bender and Jönsson (2016) and Riser and Johnson (2008)), they are either close to or higher than earlier estimates.

Our estimates suggest that prior methods have underestimated ANCP by a factor of 1.1–2.8 in the SAZ, PFZ and AZ. The underestimation factor increases to 3.7–8.2 in the less-sampled SZ, depending on basin. We suggest that our method could be more robust, for three reasons. First, we accumulated all profiles in a region to calculate a representative ANCP, rather than assuming that a smaller number of Lagrangian floats accurately represent a

19448007, 2022, 15, Downloaded from https://agupubs.onlinelibrary.wiley.com/doi/10.1029/2021GL097372 by National Health And Medical Research Council, Wiley Online Library on [18/01/2024]. See the Terms and Conditions (https://onlinelibrary.wiley.com/terms-and-conditions) on Wiley Online Library for rules of use; OA articles are governed by the applicable Creative Commons License

region. Second, our calculations used more data due to an expanding fleet, and we didn't have to exclude floats that didn't complete a seasonal cycle in the same region. Third, we compared several different depth ranges and found that on average, 14% of remineralization occurred below 500 m and 15% occurred between the euphotic depth and 100 m (Figure 3).

Using 1,000 m as the lower bound captures deep remineralization that could not be measured in previous studies that did not consider depths below 500 m (see the negative dDO/dt below 500 m, Figure 2). However, the choice of the upper boundary comes with important implications as to what is being measured. While we define ANCP as all POC available for potential export from the surface layer, we note that what is measured as ANCP depends on the definition of the surface layer. Here, we chose the greater of the euphotic depth and MLD to constrain the biologically active layer, where phytoplankton have access to light. Overall, this definition estimates ANCP 12% higher than when using 100 m, but 9% less than when using MLD (see Figure S4 in Supporting Information S1 for regional variability). Additionally, when further comparing ANCP to EP, any definition of the surface ocean is agnostic to how deep that material is exported below it or if it is exported on timescales that matter. In this sense, dissolved inorganic carbon (DIC) remineralized quickly and recirculated by deep winter mixing should be accounted for in estimates of export efficiency, but not ANCP (see Section 4.3). This definition of ANCP does not require any assumptions about the depth horizon that delineates climate-relevant timescales and enables comparison across regions with different winter mixing depths.

4.2. Potential Biases Due To Physical Processes

In locations with weak seasonality in productivity, export, and MLD, the physical variability in dDO/dt can be comparable to that due to biology, meaning observed dDO/dt may be insufficient to determine remineralization (Hennon et al., 2016). However, the Southern Ocean exhibits very strong seasonality in productivity (Buongiorno Nardelli et al., 2017), so we argue that physical processes are unlikely to bias our results, consistent with previous studies (Arteaga et al., 2019).

Spatially, our approach assumes that we can treat a specific basin and frontal zone as a homogenous whole, with no significant gradients. In reality, meridional overturning circulation, northward Ekman transport, and the formation of intermediate and mode waters carry water masses and their oxygen signatures at sub-basin scales (Downes et al., 2009). However, positive and negative DO gradients driven by water mass changes tend to cancel out in a large float array (Hennon et al., 2016; Najjar & Keeling, 1997).

Physical processes are assumed to account for the measured resupply of oxygen during winter, dominated by the ventilation of deep oxygen-depleted waters during winter mixing, where the magnitude of positive dDO/dt is largest (Figure 2). They should not dominate dDO/dt during the productive period when mixing is weak. Other processes contributing to positive winter dDO/dt, such as circulation of recently ventilated upstream water, may continue through summer. This would mean our method measures negative dDO/dt superimposed on a small background positive dDO/dt, leading to an underestimation of remineralization. Additionally, because ANCP is integrated on isobars, the seasonal deformation of isopycnals could bias our estimation of R (see Section 9 in Supporting Information S1). However, during the productive period, isopycnal movement is predominately downward, carrying higher DO water to depth and possibly leading to a further underestimation of R (Figure S6 in Supporting Information S1). We integrate from Z_{surf} (mostly equal to Z_{eu}) to 1,000 m, minimizing the effects of isopycnal movement and diapycnal diffusion between summer MLD and Z_{eu}. So, while higher than previous studies, our calculations are unlikely to be overestimates.

4.3. Southern Ocean Carbon Export

We observed higher ANCP and export than other float-based basin-scale studies in the Southern Ocean (Arteaga et al., 2019; Johnson et al., 2017), and ANCP close to or higher than some local process studies (Hennon et al., 2016; Lourey & Trull, 2001; MacCready & Quay, 2001; Martz et al., 2008; McNeil & Tilbrook, 2009; Munro et al., 2015; Shadwick et al., 2015). Considering only remineralization below 100 m to be consistent with other studies, we calculated 3.66 GT C year^{-1} of Southern Ocean carbon export, compared to 3.00 GT C year^{-1} (Schlitzer, 2002), 1.99 GT C year^{-1} (MacCready & Quay, 2001) and 2.00 GT C year^{-1} (Louanchi & Najjar, 2000), which were all integrated over larger regions than our study. However, in much of the Southern Ocean, deep winter mixing penetrates well below 100 m, meaning some of what is counted as ANCP by us and others is

recirculated back into contact with the atmosphere as DIC on times scales of 6–12 months. Accordingly, we recalculated $ANCP_{MLDwinter}$ by integrating to the climatological maximum MLD in each region. This led to an estimate of 2.79 GT C $year^{-1}$, 24% less than when using 100 m as an upper bound, and about 28% less than our Z_{surf} estimate. This challenges the common assumption that ANCP and export are equivalent at large enough space and time scales. Still, even our most conservative estimates of ANCP suggest that the Southern Ocean is playing a more important role in the global carbon cycle than previously calculated.

As shown in Figure S5 of Supporting Information S1, the large regional variability in export efficiency suggests that community composition, zooplankton grazing rates, higher trophic level pressures and microbial communities may be just as important as NPP in controlling EP (Henley et al., 2020; Le Moigne et al., 2014; Rigual Hernández et al., 2020). Consistent with Fan et al. (2020), we found the e-ratio was less than 0.5 in all basins of the SAZ and larger than 0.5 in the PFZ of the Indian and pacific sector. However, the e-ratio in the Atlantic PFZ and in all basins of the AZ was small, which contradicts Fan et al. (2020). We also found that the e-ratio doesn't always increase from north to south as temperature decreases, suggesting either temperature effect on the e-ratio is masked by variations in silica ballast (Britten et al., 2017) or grazing processes facilitate efficient export (Le Moigne et al., 2014).

5. Conclusions

Our study provides a novel approach for estimating ANCP in the Southern Ocean, based on dDO/dt observed with a large and expanding ensemble of BGC-Argo floats. By using an ensemble, our method allows for the use of roughly twice as many floats as previous float-based studies, likely enabling more representative regional estimates. Our results suggest that regional ANCP is a factor of 1.1–2.8 larger than prior estimates, in part by choosing a depth range from 100 to 500 m. Total basin-integrated ANCP in the Southern Ocean was estimated as 3.89 GT C $year^{-1}$, also higher than previous estimates. Our estimates may translate to a stronger biological pump and suggest a more important role than previously assumed for the Southern Ocean in regulating oceanic carbon storage, atmospheric CO_2, and climate. The Southern Ocean represents 30% of the ocean area but contributes 32%–78% of global ANCP (5–12 GT C yr^{-1}). As the BGC-Argo fleet expands, we might be able to resolve ANCP seasonally and annually and better reveal its temporal and spatial variability in response to climate variability and long-term change.

Data Availability Statement

The BGC-Argo float data can be downloaded from http://doi.org/10.17882/42182. The global BGC-Argo community provided the data set through the International Argo Program and the national programs that contribute to it (http://www.argo.ucsd.edu, http://argo.jcommops.org).

Acknowledgments
The Argo Program is part of the Global Ocean Observing System. We specifically acknowledge the Southern Ocean Carbon and Climate Observations and Modeling Project funded by the National Science Foundation, Division of Polar Programs (NSF PLR -1425989 and OPP-1936222), supplemented by NASA. Australian participation is supported by Australia's Integrated Marine Observing System, enabled by the National Collaborative Research Infrastructure Strategy. This research was supported by the Australian Research Council Centre of Excellence for Climate Extremes (CE170100023). HP acknowledges the Australian Government's National Environmental Science Program Climate Systems Hub. Open access publishing facilitated by University of Tasmania, as part of the Wiley - University of Tasmania agreement via the Council of Australian University Librarians.

References

Anderson, L. A., & Sarmiento, J. L. (1994). Redfield ratios of remineralization determined by nutrient data analysis. *Global Biogeochemical Cycles*, *8*(1), 65–80. https://doi.org/10.1029/93gb03318

Arteaga, L. A., Pahlow, M., Bushinsky, S. M., & Sarmiento, J. L. (2019). Nutrient controls on export production in the Southern Ocean. *Global Biogeochemical Cycles*, *33*(8), 942–956. https://doi.org/10.1029/2019gb006236

Barbieux, M., Uitz, J., Bricaud, A., Organelli, E., Poteau, A., Schmechtig, C., et al. (2018). Assessing the variability in the relationship between the particulate backscattering coefficient and the chlorophyll a concentration from a global biogeochemical-Argo database. *Journal of Geophysical Research: Oceans*, *123*, 1229–1250. https://doi.org/10.1002/2017jc013030

Bender, M. L., & Jönsson, B. (2016). Is seasonal net community production in the South Pacific Subtropical Gyre anomalously low? *Geophysical Research Letters*, *43*(18), 9757–9763. https://doi.org/10.1002/2016gl070220

Bittig, H. C., Maurer, T. L., Plant, J. N., Schmechtig, C., Wong, A. P., Claustre, H., et al. (2019). A BGC-Argo guide: Planning, deployment, data handling and usage. *Frontiers in Marine Science*, *6*, 502. https://doi.org/10.3389/fmars.2019.00502

Britten, G. L., Wakamatsu, L., & Primeau, F. W. (2017). The temperature-ballast hypothesis explains carbon export efficiency observations in the Southern Ocean. *Geophysical Research Letters*, *44*(4), 1831–1838. https://doi.org/10.1002/2016gl072378

Brix, H., Gruber, N., Karl, D. M., & Bates, N. R. (2006). On the relationships between primary, net community, and export production in subtropical gyres. *Deep Sea Research Part II: Topical Studies in Oceanography*, *53*(5–7), 698–717. https://doi.org/10.1016/j.dsr2.2006.01.024

Buongiorno Nardelli, B., Guinehut, S., Verbrugge, N., Cotroneo, Y., Zambianchi, E., & Iudicone, D. (2017). Southern Ocean mixed-layer seasonal and interannual variations from combined satellite and in situ data. *Journal of Geophysical Research: Oceans*, *122*, 10042–10060. https://doi.org/10.1002/2017jc013314

Bushinsky, S. M., & Emerson, S. R. (2018). Biological and physical controls on the oxygen cycle in the Kuroshio Extension from an array of profiling floats. *Deep Sea Research Part I: Oceanographic Research Papers*, *141*, 51–70. https://doi.org/10.1016/j.dsr.2018.09.005

19448007, 2022, 15, Downloaded from https://agupubs.onlinelibrary.wiley.com/doi/10.1029/2021GL097372 by National Health And Medical Research Council, Wiley Online Library on [18/01/2024]. See the Terms and Conditions (https://onlinelibrary.wiley.com/terms-and-conditions) on Wiley Online Library for rules of use; OA articles are governed by the applicable Creative Commons License

Cavalieri, D. J., Parkinson, C. L., Gloersen, P., & Zwally, H. J. (1996). Sea ice concentrations from Nimbus-7 SMMR and DMSP SSM/I-SSMIS passive microwave data, version 1.

Christina, L., & Passow, U. (2007). Factors influencing the sinking of POC and the efficiency of the biological carbon pump. *Deep Sea Research Part II: Topical Studies in Oceanography*, *54*(5–7), 639–658. https://doi.org/10.1016/j.dsr2.2007.01.004

Downes, S. M., Bindoff, N. L., & Rintoul, S. R. (2009). Impacts of climate change on the subduction of mode and intermediate water masses in the Southern Ocean. *Journal of Climate*, *22*(12), 3289–3302. https://doi.org/10.1175/2008jcli2653.1

Emerson, S. (2014). Annual net community production and the biological carbon flux in the ocean. *Global Biogeochemical Cycles*, *28*(1), 14–28. https://doi.org/10.1002/2013gb004680

Falkowski, P. (2012). Ocean science: The power of plankton. *Nature*, *483*(7387), S17–S20. https://doi.org/10.1038/483s17a

Fan, G., Han, Z., Ma, W., Chen, S., Chai, F., Mazloff, M. R., et al. (2020). Southern Ocean carbon export efficiency in relation to temperature and primary productivity. *Scientific Reports*, *10*(1), 1–11. https://doi.org/10.1038/s41598-020-70417-z

Giering, S. L., Sanders, R., Lampitt, R. S., Anderson, T. R., Tamburini, C., Boutrif, M., et al. (2014). Reconciliation of the carbon budget in the ocean's twilight zone. *Nature*, *507*(7493), 480–483. https://doi.org/10.1038/nature13123

Henley, S. F., Cavan, E. L., Fawcett, S. E., Kerr, R., Monteiro, T., Sherrell, R. M., et al. (2020). Changing biogeochemistry of the Southern Ocean and its ecosystem implications. *Frontiers in Marine Science*, *7*, 581. https://doi.org/10.3389/fmars.2020.00581

Hennon, T. D., Riser, S. C., & Mecking, S. (2016). Profiling float-based observations of net respiration beneath the mixed layer. *Global Biogeochemical Cycles*, *30*(6), 920–932. https://doi.org/10.1002/2016gb005380

Holte, J., & Talley, L. (2009). A new algorithm for finding mixed layer depths with applications to Argo data and Subantarctic Mode Water formation. *Journal of Atmospheric and Oceanic Technology*, *26*(9), 1920–1939. https://doi.org/10.1175/2009jtecho543.1

Honjo, S., Francois, R., Manganini, S., Dymond, J., & Collier, R. (2000). Particle fluxes to the interior of the Southern Ocean in the Western Pacific sector along 170 W. *Deep Sea Research Part II: Topical Studies in Oceanography*, *47*(15–16), 3521–3548. https://doi.org/10.1016/s0967-0645(00)00077-1

Johnson, K. S., Plant, J. N., Dunne, J. P., Talley, L. D., & Sarmiento, J. L. (2017). Annual nitrate drawdown observed by SOCCOM profiling floats and the relationship to annual net community production. *Journal of Geophysical Research: Oceans*, *122*, 6668–6683. https://doi.org/10.1002/2017jc012839

Laufkötter, C., Vogt, M., Gruber, N., Aumont, O., Bopp, L., Doney, S. C., et al. (2016). Projected decreases in future marine export production: The role of the carbon flux through the upper ocean ecosystem. *Biogeosciences*, *13*(13), 4023–4047. https://doi.org/10.5194/bg-13-4023-2016

Le Moigne, F. A., Pabortsava, K., Marcinko, C. L., Martin, P., & Sanders, R. J. (2014). Where is mineral ballast important for surface export of particulate organic carbon in the ocean? *Geophysical Research Letters*, *41*(23), 8460–8468. https://doi.org/10.1002/2014gl061678

Llort, J., Langlais, C., Matear, R., Moreau, S., Lenton, A., & Strutton, P. G. (2018). Evaluating Southern Ocean carbon eddy-pump from biogeochemical-Argo floats. *Journal of Geophysical Research: Oceans*, *123*, 971–984. https://doi.org/10.1002/2017jc012861

Louanchi, F., & Najjar, R. G. (2000). A global monthly climatology of phosphate, nitrate, and silicate in the upper ocean: Spring-summer export production and shallow remineralization. *Global Biogeochemical Cycles*, *14*(3), 957–977. https://doi.org/10.1029/1999gb001215

Lourey, M. J., & Trull, T. W. (2001). Seasonal nutrient depletion and carbon export in the subantarctic and polar frontal zones of the Southern Ocean south of Australia. *Journal of Geophysical Research*, *106*(C12), 31463–31487. https://doi.org/10.1029/2000jc000287

MacCready, P., & Quay, P. (2001). Biological export flux in the Southern Ocean estimated from a climatological nitrate budget. *Deep Sea Research Part II: Topical Studies in Oceanography*, *48*(19–20), 4299–4322. https://doi.org/10.1016/s0967-0645(01)00090-x

Martz, T. R., Johnson, K. S., & Riser, S. C. (2008). Ocean metabolism observed with oxygen sensors on profiling floats in the South Pacific. *Limnology & Oceanography*, *53*(5part2), 2094–2111. https://doi.org/10.4319/lo.2008.53.5_part_2.2094

McDougall, T. J., & Barker, P. M. (2011). Getting started with TEOS-10 and the Gibbs Seawater (GSW) oceanographic toolbox. *SCOR/IAPSO WG*, *127*, 1–28.

McNeil, B., & Tilbrook, B. (2009). A seasonal carbon budget for the sub-Antarctic Ocean, South of Australia. *Marine Chemistry*, *115*(3–4), 196–210. https://doi.org/10.1016/j.marchem.2009.08.006

Morel, A., & Maritorena, S. (2001). Bio-optical properties of oceanic waters: A reappraisal. *Journal of Geophysical Research*, *106*(C4), 7163–7180. https://doi.org/10.1029/2000jc000319

Munro, D. R., Lovenduski, N. S., Stephens, B. B., Newberger, T., Arrigo, K. R., Takahashi, T., et al. (2015). Estimates of net community production in the Southern Ocean determined from time series observations (2002–2011) of nutrients, dissolved inorganic carbon, and surface ocean pCO2 in Drake Passage. *Deep Sea Research Part II: Topical Studies in Oceanography*, *114*, 49–63. https://doi.org/10.1016/j.dsr2.2014.12.014

Najjar, R. G., & Keeling, R. F. (1997). Analysis of the mean annual cycle of the dissolved oxygen anomaly in the World Ocean. *Journal of Marine Research*, *55*(1), 117–151. https://doi.org/10.1357/0022240973224481

Nicholson, D., Emerson, S., & Eriksen, C. C. (2008). Net community production in the deep euphotic zone of the subtropical North Pacific gyre from glider surveys. *Limnology & Oceanography*, *53*(5part2), 2226–2236. https://doi.org/10.4319/lo.2008.53.5_part_2.2226

Rigual Hernández, A. S., Trull, T. W., Nodder, S. D., Flores, J. A., Bostock, H., Abrantes, F., et al. (2020). Coccolithophore biodiversity controls carbonate export in the Southern Ocean. *Biogeosciences*, *17*(1), 245–263. https://doi.org/10.5194/bg-17-245-2020

Riser, S. C., & Johnson, K. S. (2008). Net production of oxygen in the subtropical ocean. *Nature*, *451*(7176), 323–325. https://doi.org/10.1038/nature06441

Sabine, C. L., Feely, R. A., Gruber, N., Key, R. M., Lee, K., Bullister, J. L., et al. (2004). The oceanic sink for anthropogenic CO2. *Science*, *305*(5682), 367–371. https://doi.org/10.1126/science.1097403

Sarmiento, J. L., & Gruber, N. (2002). Sinks for anthropogenic carbon. *Physics Today*, *55*(8), 30–36. https://doi.org/10.1063/1.1510279

Schlitzer, R. (2002). Carbon export fluxes in the Southern Ocean: Results from inverse modeling and comparison with satellite-based estimates. *Deep Sea Research Part II: Topical Studies in Oceanography*, *49*(9–10), 1623–1644. https://doi.org/10.1016/s0967-0645(02)00004-8

Shadwick, E., Trull, T., Tilbrook, B., Sutton, A., Schulz, E., & Sabine, C. (2015). Seasonality of biological and physical controls on surface ocean CO2 from hourly observations at the Southern Ocean Time Series site south of Australia. *Global Biogeochemical Cycles*, *29*(2), 223–238. https://doi.org/10.1002/2014gb004906

Steinberg, D. K., Van Mooy, B. A., Buesseler, K. O., Boyd, P. W., Kobari, T., & Karl, D. M. (2008). Bacterial vs. zooplankton control of sinking particle flux in the ocean's twilight zone. *Limnology & Oceanography*, *53*(4), 1327–1338. https://doi.org/10.4319/lo.2008.53.4.1327

Su, J., Strutton, P. G., & Schallenberg, C. (2021). The subsurface biological structure of Southern Ocean eddies revealed by BGC-Argo floats. *Journal of Marine Systems*, *220*, 103569. https://doi.org/10.1016/j.jmarsys.2021.103569

Talley, L. D. (2011). *Descriptive physical oceanography: An introduction*. Academic press.

Westberry, T., Behrenfeld, M., Siegel, D., & Boss, E. (2008). Carbon-based primary productivity modeling with vertically resolved photoacclimation. *Global Biogeochemical Cycles*, *22*(2), GB2024. https://doi.org/10.1029/2007gb003078

19448007, 2022, 15, Downloaded from https://agupubs.onlinelibrary.wiley.com/doi/10.1029/2021GL097372 by National Health And Medical Research Council, Wiley Online Library on [18/01/2024]. See the Terms and Conditions (https://onlinelibrary.wiley.com/terms-and-conditions) on Wiley Online Library for rules of use; OA articles are governed by the applicable Creative Commons License

Williams, N., Juranek, L., Feely, R., Russell, J., Johnson, K., & Hales, B. (2018). Assessment of the carbonate chemistry seasonal cycles in the Southern Ocean from persistent observational platforms. *Journal of Geophysical Research: Oceans*, *123*, 4833–4852. https://doi.org/10.1029/2017jc012917

Xing, X., Claustre, H., Blain, S., d'Ortenzio, F., Antoine, D., Ras, J., & Guinet, C. (2012). Quenching correction for in vivo chlorophyll fluorescence acquired by autonomous platforms: A case study with instrumented elephant seals in the Kerguelen region (Southern Ocean). *Limnology and Oceanography: Methods*, *10*(7), 483–495. https://doi.org/10.4319/lom.2012.10.483

Yang, B., Emerson, S. R., & Bushinsky, S. M. (2017). Annual net community production in the subtropical Pacific Ocean from in situ oxygen measurements on profiling floats. *Global Biogeochemical Cycles*, *31*(4), 728–744. https://doi.org/10.1002/2016gb005545

19448007, 2022, 15, Downloaded from https://agupubs.onlinelibrary.wiley.com/doi/10.1029/2021GL097372 by National Health And Medical Research Council, Wiley Online Library on [18/01/2024]. See the Terms and Conditions (https://onlinelibrary.wiley.com/terms-and-conditions) on Wiley Online Library for rules of use; OA articles are governed by the applicable Creative Commons License